Journal of Catalysis **185,** 213–218 (1999)
Article ID jcat.1999.2512, available online at http://www.idealibrary.com on IDEAL®

# The Dynamics of Oxygen Exchange with Zirconia-Supported PdO

Jacky Au-Yeung,* Alexis T. Bell,†,[1] and Enrique Iglesia‡,[1]

†*Chemical Sciences Division and* ‡*Material Sciences Division, Lawrence Berkeley National Laboratory, and* **Department of Chemical Engineering, University of California at Berkeley, Berkeley, California 94720-1462*

Received January 13, 1999; revised March 29, 1999; accepted March 30, 1999

**Isotopic tracer methods involving $^{18}O$ and $^{16}O$ were used to investigate the dynamics of $O_2$ adsorption and desorption from the surface of zirconia-supported PdO and the dynamics of O atom diffusion through the bulk of PdO. The rate coefficient for the recombination of O atoms is found to be $1.4 \times 10^{13}$ exp(−144,000/RT) $s^{-1}$ and the diffusivity of O atoms through bulk PdO is $1.6 \times 10^{-10}$ exp(−89,000/RT) $cm^2/s$. In both cases, the activation energies are in units of kJ/mol. While oxygen exchange with pure $ZrO_2$ was not observed under the conditions of the present experiments, such exchange did occur to a limited degree when PdO was supported on $ZrO_2$, the degree of exchange increasing with decreasing PdO particle size.** 

## INTRODUCTION

Palladium oxide supported on zirconia is known to be a particularly active catalyst for the combustion of methane (1–6). Analysis of the reaction kinetics suggests that dissociatively adsorbed $CH_4$ reacts with oxygen atoms present at the surface of PdO particles. The oxygen lost from the catalyst is replenished by dissociative adsorption of $O_2$ from the gas phase and by diffusion from the catalyst bulk. For this reason it is of interest to measure the dynamics of oxygen adsorption and desorption, as well as the dynamics of oxygen diffusion through bulk PdO. The dynamics of both processes were investigated in the present study by means of isotopic tracer techniques. While this approach has been used previously to study oxygen exchange between gas phase $O_2$ and a metal oxide (7–12), its application to PdO has been reported only once before (7b).

## EXPERIMENTAL

The $PdO/ZrO_2$ catalyst was prepared by incipient wetness impregnation. Pure $ZrO_2$ (RC-100P, Daichi Kigenso Kagaku Kogyo Co.), used as the support, was heated in air from room temperature to 1073 K at a rate of 0.33 K/s. The support was held at this temperature for 24 h and then cooled to room temperature. After calcination, the $N_2$ BET surface area of the support was 16–25 $m^2/g$. The calcined support was impregnated with an aqueous solution of $Pd(NO_3)_2$ (10 wt% solution in 10 wt% nitric acid, Aldrich) to the point of incipient wetness and then dried in air for 1–2 h. These catalysts were heated from room temperature to 523 K in air at 0.0083 K/s to prevent rapid decomposition of $Pd(NO_3)_2$ (6). Subsequently, the temperature was increased at 0.17 K/s up to 773 K and then held at this temperature for 10 h before cooling down to room temperature. The Pd concentration (7.9%) was determined by elemental analysis.

Isotopic tracer studies were carried out in a cylindrical microreactor. The reactor was 250 mm long and had an inner diameter of 4 mm at both the inlet and the outlet. The center of the reactor was 8 mm wide and contained a quartz frit to support the catalysts. The reactor was heated by an electrical furnace connected to a temperature controller (CN2012, Omega). Gas was provided to the reactor from a flow manifold. The flow rate of each gas was regulated by electronic flow controllers (Tylan FC-280, RO-28). A quadrupole mass spectrometer (UTI Model 100C) was used to analyze the reactor effluent.

Dispersion was measured by $H_2$–$O_2$ titration at 373 K (8). The catalyst was first reduced in mixture of 25% $H_2$ (99.9% purity, Airco) in He (UHP Grade, Middleton Bay Airgas) flowing at 0.33 $cm^3/s$ and then purged in pure He for 0.5 h. Then the gas stream was changed to 20% $O_2$ in He (premixed, Middleton Bay Airgas). At 373 K, a single monolayer of palladium oxide was formed at an oxygen partial pressure of less than 46.7 kPa (13). Finally, pulses of 0.4 $cm^3$ of $H_2$ were passed through the reactor to titrate the surface oxygen atoms until no further consumption of $H_2$ was detected by mass spectrometry. The dispersion of Pd (14%) was calculated on the basis of the following stoichiometry (13):

$$\text{Oxidation} \qquad Pd_{(s)} + 1/2O_{2(g)} \rightarrow PdO_{(s)}$$

$$\text{Reduction} \qquad PdO_{(s)} + 3/2H_{2(g)} \rightarrow PdH_{(s)} + H_2O_{(g)}.$$

The average Pd particle size, calculated from the dispersion by assuming Pd particles are hemispherical, was 6.4 nm.

[1] To whom correspondence should be addressed. E-mail: bell@cchem.berkeley.edu.



0021-9517/99 $30.00

Temperature-programmed isotopic exchange (TPIE) of the oxygen in PdO was carried out in the following manner. The catalyst (~0.5 g) was first heated in $^{16}O_2$ (2% $^{16}O_2$ in He flowing at 1.7 cm$^3$/s) at 673 K for 1 h. The temperature was then decreased to 373 K; and the flow of $^{16}O_2$/He was replaced by $^{18}O_2$/He (99% purity, Isotec) at the same flow rate. After a period of 300 s, the catalyst temperature was increased to 673 K at a rate of 10 K/min. Gas phase concentrations of $^{16}O_2$, $^{16}O^{18}O$, and $^{18}O_2$ (Masses 32, 34, and 36) were monitored continuously by mass spectrometry.

Isotopic exchange of oxygen under isothermal condition was carried out in a manner similar to that used for the temperature-programmed experiment. The catalyst was first exposed to a flow of $^{16}O_2$/He and then replaced by a $^{18}O_2$/He mixture. Gas phase concentrations were measured by mass spectrometry downstream of the reactor. The gas phase was switched back to $^{16}O_2$ 600 s after the initial isotope switch when appreciable changes were no longer observed in the concentration of any of the oxygen isomers.

## METHODS OF DATA ANALYSIS

At the conditions of the present experiments, the reactor can be modeled as a continous-stirred tank reactor, since the particle Peclet number is 0.06, indicating a high degree of axial dispersion (14–16). Species balance equations are used to relate the mole fraction of each molecular oxygen species in the gas phase ($y_{A_2}$, $y_{AB}$, and $y_{B_2}$) to the mole fraction of atomic oxygen on the catalyst surface ($x_{A,s}$). Note that throughout this paper for simplicity, we designate species $^{16}O$ and $^{18}O$ as "A" and "B", respectively. Therefore, $A_2$ stands for $^{16}O_2$ and so forth.

Equation [1] represents the species balance for $^{16}O_2$ at each time after the isotopic switch from $A_2$ to $B_2$. In this equation, $V$, is the reactor volume, $\varepsilon$ is the reactor void fraction, $Q$ is the volumetric flowrate of gas, $C_{O_2,g}$ is the concentration of $O_2$ in the gas phase, $c_{O,s}$ and $c_v$ are the surface concentrations of oxygen and vacancies, $k_1$ and $k_{-1}$ are the rate coefficients for adsorption and desorption of $O_2$, and $x_{A,s}$ is the fraction of atomic oxygen in the form of A ($^{16}O$) at the surface of the catalyst:

$$-\varepsilon V C_{O_2,g}\frac{dy_{A_2}}{dt} = QC_{O_2,g}y_{A_2} - k_{-1}c_{O,s}^2x_{A,s}^2(1-\varepsilon)V + k_1C_{O_2,g}y_{A_2}c_v^2(1-\varepsilon)V. \quad [1]$$

The three terms on the right-hand side of Eq. [1] represent the molar flow rate of oxygen out of reactor, the rate of $^{16}O_2$ desorption, and the rate of $^{16}O_2$ readsorption. The species balance equations for AB and $B_2$ are similar:

$$-\varepsilon V C_{O_2,g}\frac{dy_{AB}}{dt} = QC_{O_2,g}y_{AB} - 2k_{-1}c_{O,s}^2x_{A,s}x_{B,s}(1-\varepsilon)V + k_1C_{O_2,g}y_{AB}c_v^2(1-\varepsilon)V \quad [2]$$

$$-\varepsilon V C_{O_2,g}\frac{dy_{B_2}}{dt} = (y_{B_2}-1)QC_{O_2,g} - k_{-1}c_{O,s}^2x_{B,s}^2(1-\varepsilon)V + k_1C_{O_2,g}y_{B_2}c_v^2(1-\varepsilon)V. \quad [3]$$

The isotopic composition of the gas phase in the reactor is assumed to change very slowly during most of the isotope-exchange period so that a pseudo-steady-state approximation is valid. Our experimental data demonstrated that the magnitude of the left-hand side of Eqs. [1]–[3] is small compared to the magnitudes of the terms appearing on the right-hand side of these equations. Setting the left-hand side of Eqs. [1]–[3] to zero and rearranging the remaining terms lead to equations for $y_{A_2}$, $y_{AB}$, and $y_{B_2}$ in terms of $x_{A,s}$,

$$y_{A_2} = \frac{Da}{1+Da}x_{A,s}^2 \quad [4]$$

$$y_{AB} = \frac{2Da}{1+Da}x_{A,s}(1-x_{A,s}) \quad [5]$$

$$y_{B_2} = 1 - \frac{Da}{1+Da}x_{A,s}(2-x_{A,s}), \quad [6]$$

where $Da = \frac{k_1C_{O_2,g}c_v^2(1-\varepsilon)V}{QC_{O_2,g}} = \frac{k_{-1}C_{O,s}^2(1-\varepsilon)V}{QC_{O_2,g}}$ is the Damkohler number for a second-order irreversible reaction (14).

Equation [5] shows that the fraction of $O_2$ present as $^{16}O^{18}O$ in the gas phase ($y_{AB}$) will be a maximum when the surface is equally covered with $^{16}O$ and $^{18}O$ ($x_{A,s}=0.5$).

Isotopic exchange of $^{18}O$ for $^{16}O$ in the bulk of the PdO particles requires intraparticle diffusion. Assuming the PdO particles to be spherical with a radius $R$, the rate at which the isotopic fraction of oxygen exchanges is governed by the diffusion equation (14)

$$c_{O,b}\frac{\partial x_A}{\partial t} = \mathcal{D}_{AB}c_{O,b}\left(\frac{\partial^2 x_A}{\partial r^2} + \frac{2}{r}\frac{\partial x_A}{\partial r}\right), \quad [7]$$

where $c_{O,b}$ is the concentration of O in bulk PdO, $x_A$ is the fraction of O in the bulk phase that is A. $r$ is the radial distance from the center of the spherical catalyst while $t$ is the elapsed time after the isotopic switch was made, and $\mathcal{D}_{AB}$ is the diffusivity of oxygen in PdO.

Equation [7] can be nondimensionalized by defining

$$r^* = \frac{r}{R}$$

and

$$t^* = \frac{t\mathcal{D}_{AB}}{L^2}. \quad [8]$$

Substituting Eq. [8] into Eq. [7] gives

$$\frac{\partial x_A}{\partial t^*} = \frac{\partial^2 x_A}{\partial r^{*2}} + \frac{2}{r^*}\frac{\partial x_A}{\partial r^*}. \quad [9]$$

The boundary condition on Eq. [9] is $\frac{\partial x_A}{\partial r^*}|_{r^*=0} = 0$ at $r^*=0$. The boundary condition at $r^*=1$ is defined by setting the

rate of A diffusion at the particle surface to the net rate at which A is removed from the surface by desorption steps ($2A \rightarrow A_{2(g)}$ and $A_s + B_s \rightarrow AB_{(g)}$). Therefore,

$$-4\pi R^2 \mathcal{D}_{AB} c_{O,b} \left.\frac{\partial x_A}{\partial r}\right|_{r=R} = \left(2\alpha y_{A_2} + 2\alpha y_{AB}\right) \frac{4}{3}\pi R^3, \quad [10]$$

where $\alpha = k_1 C_{O_2,g} c_v^2 = k_{-1} c_{O,s}^2$ because the rates of oxygen adsorption and desorption are equivalent since isotopic exchange occurs under equilibrium conditions.

Taking $c_{O,b} = \frac{c_{O,s}}{\sigma}$ ($\sigma$ is the thickness of a monolayer of PdO), and substituting for $y_{A_2}$ and $y_{AB}$ from Eqs. [4] and [5], respectively, allows Eq. [10] to be rewritten as follows:

$$\left.\frac{\partial x_A}{\partial r}\right|_{r=R} = \frac{2\alpha R}{3\mathcal{D}_{AB} c_{O,b}(1 + Da)} x_A \quad [11]$$

or

$$\left.\frac{\partial x_A}{\partial r^*}\right|_{r^*=1} = \frac{2\alpha\sigma R^2}{3\mathcal{D}_{AB} c_{O,s}(1 + Da)} x_A. \quad [12]$$

The initial condition is $x_A = 1$ for all $r^*$ at $t^* = 0$, because PdO is initially $Pd^{16}O$.

The solution for Eq. [9] with the boundary conditions and the initial condition specified above is derived in the Appendix. The final expression for $x_A$ is

$$x_A = \sum_{\text{all } \lambda} c_\lambda e^{-\lambda t^*} \frac{\sin\left(\sqrt{\lambda} r^*\right)}{r^*}, \quad [13]$$

where

$$c_\lambda = \frac{4\left(\sin\sqrt{\lambda} - \sqrt{\lambda}\cos\sqrt{\lambda}\right)}{2\lambda - \sqrt{\lambda}\sin\left(2\sqrt{\lambda}\right)}. \quad [14]$$

The eigenvalues, $\lambda$, are given by the roots of

$$\frac{\tan\sqrt{\lambda} - \sqrt{\lambda}}{\tan\sqrt{\lambda}} = \frac{2\alpha\sigma R^2}{3\mathcal{D}_{AB} c_{O,s}(1 + Da)} \equiv \Gamma. \quad [15]$$

Note that the value of $x_{A,s}$ can be found from Eq. [13] by setting $x_{A,s} = x_A(r^* = 1)$.

## RESULTS AND DISCUSSION

Figure 1 illustrates the effect of temperature on the rate of oxygen isotope exchange between $^{18}O_2$ in the gas phase and small particles of $Pd^{16}O$ supported on $ZrO_2$. In this experiment the catalyst was pretreated in $^{16}O_2$ for 1 h at 673 K, the temperature was decreased to 373 K, and $^{16}O_2$ was replaced by $^{18}O_2$ at the same concentration and flow rate. The temperature was then increased at 0.17 K/s to 673 K. Below 550 K, the consumption of $^{18}O_2$ and the production of $^{16}O^{18}O$ were not detected, indicating very low isotope exchange rates. Between 550 and 673 K, the rate of isotopic exchange increases, and at the highest temperature, approximately a quarter of the $^{16}O$ originally present in the PdO has been replaced by $^{18}O$.

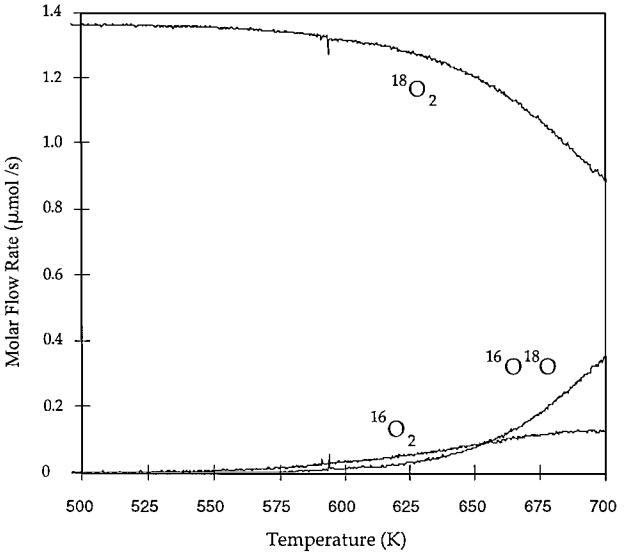


**FIG. 1.** Temperature-programmed isotopic exchanges of oxygen [2% $^{18}O_2$ in He flowing at 100 $cm^3$/min; 0.528 g 7.9% $PdO/ZrO_2$].

Turnover rates for $^{18}O_2$ consumption per exposed Pd atom are plotted in the Arrhenius plot of Fig. 2. The slope of this Arrhenius plot gives an apparent activation energy of 84 kJ/mol. As shown below, this value is approximately equal to the activation energy for oxygen diffusion through PdO. Similar measurements were also made for $Pd/ZrO_2$ catalysts prepared with higher loadings of Pd. Table 1 illustrates the effects of Pd loading and, more importantly, Pd dispersion on the activation energy for $^{18}O_2$ consumption. The decrease in apparent activation energy with decreasing Pd dispersion is attributed to a weakening of Pd–O bonds

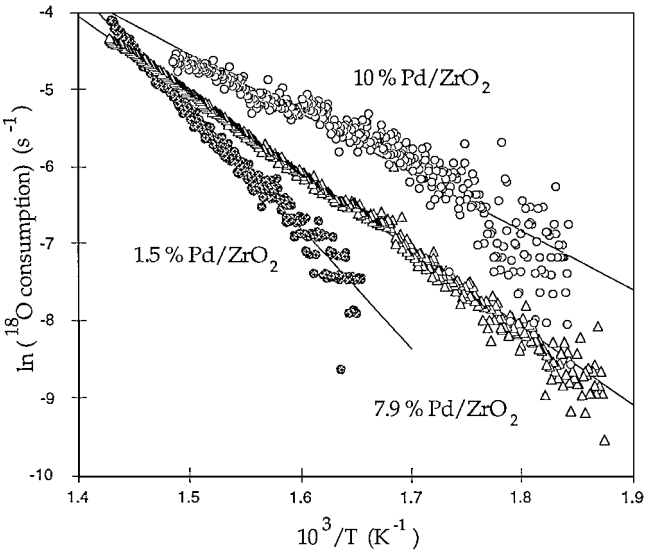


**FIG. 2.** Arrhenius plot of oxygen TPIE [2% $^{18}O_2$ in He flowing at 100 $cm^3$/min; 0.5 g catalysts].

**TABLE 1**

**Effects of Pd Dispersion on the Apparent Activation Energy for Oxygen Diffusion**

| Pd loading (%) | Pd dispersion (%) | $E_a$ (kJ/mol) |
|---|---|---|
| 1.46 | 23 | 128 |
| 7.87 | 14 | 84 |
| 10 | 4 | 64 |

with increasing PdO particle size, enabling diffusion to occur more rapidly (17). Similar arguments have been used to explain the increase in the turnover frequency for $CH_4$ combustion over supported PdO (6). It should also be noted that the apparent activation energies reported in Table 1 are in rough agreement with the value reported earlier for bulk PdO, $86 \pm 13$ kJ/mol (7b).

Isothermal isotope-exchange experiments were conducted on pure $ZrO_2$ in order to establish if the support contributes to the isotopic exchange rates measured on $PdO/ZrO_2$. These experiments were conducted at temperatures from 613 to 693 K. In all cases, both the Ar and the $^{16}O_2$ signals fell to zero in 5 s, after the switch had been made from a stream containing 2% $^{16}O_2$ and 1% Ar (balance He) to one containing 2% $^{18}O_2$ (balance He). The identical $^{16}O_2$ and Ar decay curves and the absence $^{16}O^{18}O$ show that isotopic exchange of oxygen between the gas phase and the support does not occur in the absence of PdO.

The results of similar experiments on the $PdO/ZrO_2$ at 673 K are presented in Fig. 3. As shown in the inset, the Ar signal again drops to zero within the first 5 s of the experiment, but $^{16}O_2$ and $^{18}O_2$ concentrations change much more slowly. A slow response is also observed for the $^{16}O^{18}O$ concentration, which rises to a maximum after about 60 s and then slowly decreases. The slow portions of the transients for $^{16}O_2$ and $^{18}O_2$ and the transient for $^{16}O^{18}O$ provide clear evidence for the occurrence of isotopic exchange between oxygen in the gas phase and in PdO.

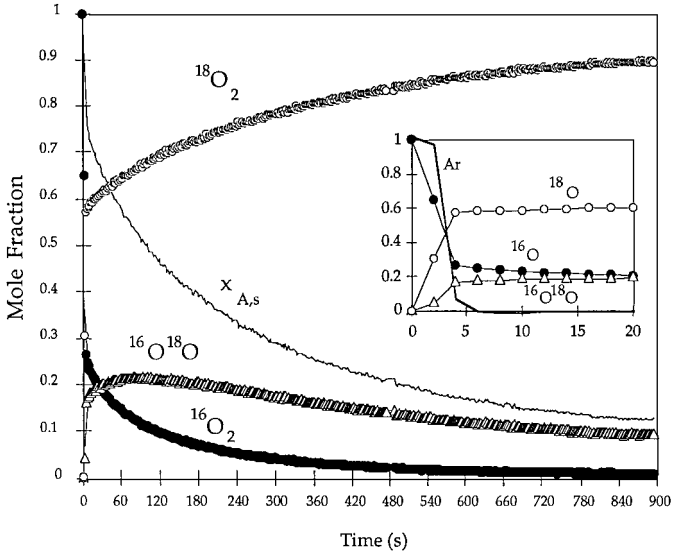


**FIG. 3.** Dynamics of oxygen isotopic exchanges at 673 K [2% $^{18}O_2$, 1% Ar in He flowing at 100 cm$^3$/min; 0.528 g 7.9% $PdO/ZrO_2$].

The mole fractions of $^{16}O_2$, $^{16}O^{18}O$, and $^{18}O_2$ were fitted simultaneously to Eqs. [4]–[6] by the least-squares method to determine $x_{A,s}$ (t) and Da. The resulting plot of $x_{A,s}$ versus time is shown in Fig. 3, as are the corresponding plots of $y_{A_2}$, $y_{AB}$, and $y_{B_2}$ versus time. The error in the fitting is minimal as the fitted curves completely overlap with the data points.

Table 2 lists the values of $\alpha$ determined from the values of Da measured at between 613 and 693 K. The temperature dependence of $\alpha$ ($\alpha = k_{-1}c_{O,s}^2$) predominantly reflects the temperature dependence of $k_{-1}$ because the surface concentration of oxygen is always the same by definition because it is in chemical equilibrium with the gas phase. Therefore, the activation energy for associative recombination of O atoms is calculated to be 144 kJ/mol. If it is further assumed that $c_{O,s} = 10^{15}$ atoms/cm$^2$, then the preexponential factor associated with $k_{-1}$ is $1.4 \times 10^{13}$ s$^{-1}$, a reasonable value for associative recombination (18).

Figure 3 shows that $x_{A,s}$ declines rapidly from 1 to 0.75 and more slowly thereafter. The initial transient is attributed to the rapid exchange of $^{16}O$ for $^{18}O$ at the surface of the supported PdO particles. As PdO surfaces are depleted of $^{16}O$, the rate of $^{16}O$ diffusion from the bulk increases, and the rate of $^{16}O$ evolution from PdO decreases. The diffusivity for oxygen through PdO can be obtained by analysis of a plot of the mole fraction of $^{16}O$ content at the PdO surface, $x_{A,s}$, versus the average mole fraction of $^{16}O$ in PdO, $\bar{x}_A$. Plots of $x_{A,s}$ versus $\bar{x}_A$ are shown in Fig. 4 for temperatures of 653, 673, and 693 K. The value of $x_{A,s}$ should approach zero as $\bar{x}_A$ goes to zero. The observation of a nonzero intercept for all temperatures suggests the existence of a pool of $^{16}O$ that contributes to isotopic exchange after all of the $^{16}O$ in PdO is consumed. One possibility is that the presence of PdO particles facilitates the exchange of oxygen with the $ZrO_2$ support. If this were the case, the deviation from a nonzero intercept should become more severe as the PdO

**TABLE 2**

**Mass-34 Maximum Intensity for Steady State Isotopic Exchange for 7.9% $PdO/ZrO_2$ catalyst**

| $T$ (K) | $y_{AB,\,max}$ | Time after switch (s) | $O_2$ exchange rate (mol $O_2$/m$^2$/s) |
|---|---|---|---|
| 613 | 0.02 | 275 | $9.0 \times 10^{-2}$ |
| 633 | 0.09 | 270 | $4.2 \times 10^{-4}$ |
| 653 | 0.12 | 200 | $5.8 \times 10^{-4}$ |
| 673 | 0.22 | 100 | $1.4 \times 10^{-3}$ |
| 693 | 0.30 | 87 | $2.8 \times 10^{-3}$ |

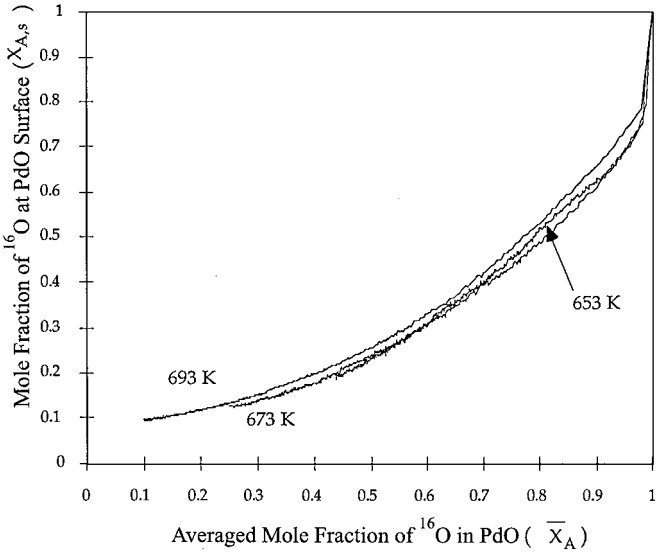


**FIG. 4.** Plot of mole fraction of $^{16}$O at the surface of PdO particles versus averaged mole fraction of $^{16}$O in the bulk of the PdO particles.

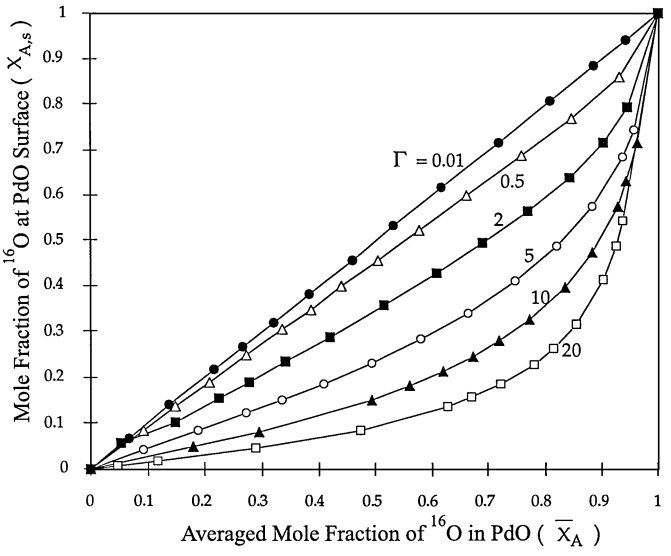


**FIG. 6.** Plot of mole fraction of $^{16}$O at the surface of PdO particles versus averaged mole fraction of $^{16}$O in the bulk of the PdO particles based on theoretical model of oxygen exchange.

particle size decreases. Consistent with this hypothesis, it was observed (data not shown) that the *y*-intercept was as high as 0.5 for isotopic exchanges on a 2.5% $PdO/ZrO_2$ catalyst (19% dispersion). A similar effect of particle size has been reported for Rh supported on $Al_2O_3$ (19, 20), where it was observed that small Rh particles facilitate oxygen exchange with the support.

The model of oxygen atom transport through PdO and isotopic exchange at the particle surface, described by Eqs. [9]–[15], can be used to generate a theoretical plot of $x_{A,s}$ versus $\bar{x}_A$. The first step is to generate a theoretical plot of $x_A(r^*)$ for different times after the onset of an isotope-exchange experiment. Figure 5 shows such plots for

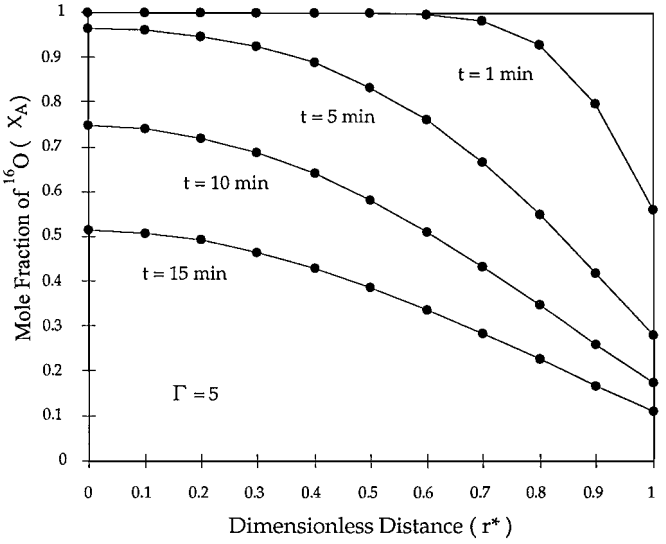


**FIG. 5.** Isotopic distribution of oxygen in PdO particles as a function of radial distance.

$\Gamma = 5$. In this case, the value of $x_{A,s}$ drops rapidly from unity to 0.6 during the first minute, while the interior of the PdO particle retains a value of $x_A = 1$. After about 5 min, the extent of $^{16}$O depletion becomes sufficient for the value of $x_{A,s}$ within the particle to slowly decline with time.

A plot of $x_{A,s}$ versus $\bar{x}_A$ is generated by determining $\bar{x}_A$ for a given time from the integral of the the corresponding curve of $x_A(r^*)$. Figure 6 shows a plot of $x_{A,s}$ versus $\bar{x}_A$ for different values of $\Gamma$. The shapes of these curves are similar to that seen in Fig. 4; and close agreement between theory and experiment is achieved when $\Gamma = 5$. From this value of $\Gamma$, it is determined that $\mathcal{D}_{AB} = 1.6 \times 10^{-10}$ exp(−89,000/RT) $cm^2/s$. The activation energy for diffusion, 89 kJ/mol, determined in this fashion is very close to the value of the apparent activation energy for isotopic exchange, 84 kJ/mol, determined from Fig. 2. The reason for this agreement becomes apparent once it is recognized that the net rate of $^{18}O_2$ consumption per unit area of PdO particle surface, $\bar{r}_{O_2} = \mathcal{D}_{AB} c_{O,b} \frac{\partial x_A}{\partial r}|_{r=R}$. If it is assumed that $c_{O,s}$ and the gradient in $x_{A,s}$ are not strongly temperature dependent, then $\mathcal{D}_{AB}$ is the sole factor on the right-hand side of the equation exhibiting a temperature dependence.

## CONCLUSIONS

The dynamics of oxygen exchange with PdO supported on $ZrO_2$ were investigated by isotopic tracer methods. The rate coefficient for recombination of O atoms at the surface of PdO is found to be $1.4 \times 10^{13}$ exp(−144,000/RT) $s^{-1}$ and the diffusivity for O atoms diffusing through PdO is $1.6 \times 10^{-10}$ exp(−89,000/RT) $cm^2/s$. While oxygen exchange with pure $ZrO_2$ was not observed, evidence for such

exchange was seen in the presence of PdO. The extent to which PdO facilitates exchange of O with $ZrO_2$ increases with decreasing size of the PdO particles.

## APPENDIX: DERIVATION OF SOLUTION FOR DIFFUSION EQUATION

We start the derivation by separating the variables $r^*$ and $t^*$:

$$x_A = R(r^*)\Theta(t^*). \quad [16]$$

Substitution of Eq. [16] into Eq. [9] leads to

$$\frac{\dot{\Theta}}{\Theta} = \frac{R''}{R} = -\lambda. \quad [17]$$

The solution to Eq. [17] is

$$\Theta = g_1 e^{-\lambda t^*}$$
$$R = g_2 \frac{\sin\sqrt{\lambda} r^*}{r^*} + g_3 \frac{\cos\sqrt{\lambda} r^*}{r^*}. \quad [18]$$

The first boundary condition suggests that the isotope concentration is finite; it implies that

$$g_3 = 0, \quad [19]$$

since

$$\lim_{r^* \to 0} \frac{\cos\sqrt{\lambda} r^*}{r^*} \to \infty. \quad [20]$$

The second boundary condition (Eq. [12]) requires that

$$\left.\frac{\partial x_A}{\partial r^*}\right|_{r^*=1} = g_2\Theta(\sqrt{\lambda}\cos\sqrt{\lambda} - \sin\sqrt{\lambda})$$
$$= \frac{-2\alpha\sigma R^2}{3\mathcal{D}_{AB} c_{O,s}(1 + Da)} g_2 \Theta \sin\sqrt{\lambda}. \quad [21]$$

Equation [21] can be rewritten as a transdendal equation to relate eigenvalues and physical parameters such as $\alpha$, $\beta$, and $\mathcal{D}_{AB}$:

$$\frac{\tan\sqrt{\lambda} - \sqrt{\lambda}}{\tan\sqrt{\lambda}} = \frac{2\alpha\sigma R^2}{3\mathcal{D}_{AB} c_{O,s}(1 + Da)} \equiv \Gamma. \quad [15]$$

Since any eigenvalue which satisfies Eq. [15] is a valid solution for Eq. [18], the summation of all solutions which contain distinct eigenvalues must also be a valid solution. Therefore,

$$x_A = \sum_{\text{all } \lambda} c_\lambda e^{-\lambda t^*} \frac{\sin\sqrt{\lambda} r^*}{r^*}. \quad [13]$$

Finally, we have to determine $c_\lambda$. The initial condition requires that

$$x_A\big|_{t^*=0} = \sum_{\text{all } \lambda} c_\lambda \frac{\sin\sqrt{\lambda} r^*}{r^*} = 1. \quad [22]$$

To determine $c_\lambda$, we can multiply Eq. [23] by $r^* \sin\sqrt{\lambda} r^*$ and integrate $r^*$ from 0 to 1. After combining terms and algebraic rearrangements, we find

$$c_\lambda = \frac{4(\sin\sqrt{\lambda} - \sqrt{\lambda}\cos\sqrt{\lambda})}{2\lambda - \sqrt{\lambda}\sin(2\sqrt{\lambda})}. \quad [14]$$

.

## ACKNOWLEDGMENTS

This work was supported by a grant from the American Chemical Society, Petroleum Research Fund. Equipment was made available by the Office of Basic Energy Sciences, Chemical Sciences Divison of the U.S. Department of Energy under Contract DE-AC03-76SF00098.

## REFERENCES

1. Ribeiro, F. H., Chow, M., and Dalla Betta, R. A., *J. Catal.* **146**, 537 (1994).
2. Burch, R., and Hayes, M. J., *J. Mol. Catal. A: Chem.* **100**, 13 (1995).
3. Muller, C. A., Maciejewski, M., Koeppel, R. A., Tschan, R., and Baiker, A., *J. Phys. Chem.* **100**, 20006 (1996).
4. Carstens, J. N., Su, S. C., and Bell, A. T., *J. Catal.* **176**, 136 (1998).
5. Muller, C. A., Maciejewski, M., Koeppel, R. A., and Baiker, A., *J. Catal.* **166**, 36 (1997).
6. Fujimoto, K., Ribeiro, F. H., Avalos-Borja, M., and Iglesia, E., *J. Catal.* **179**, 431 (1998).
7. Winter, E. R. S., (a) *J. Chem. Soc.* 1170 (1950); (b) *J. Chem. Soc.* **1**, 2889 (1968); (c) *Adv. Catal.* **15**, 285 (1964).
8. Boreskov, G. K., *Adv. Catal.* **15**, 285 (1968).
9. Boreskov, G. K., and Muzykantov, V. S., *Ann. NY Acad. Sci.* **213**, 137 (1973).
10. Novakova, J., *Catal. Rev.* **4**, 77 (1970).
11. Klier, K., Novakova, J., and Jiru, P. J., *J. Catal.* **2**, 479 (1963).
12. Holmgren, A., Duprez, D., and Andersson, B., *J. Catal.* **182**, 441 (1999).
13. Benson, J. E., Hwang, H. S., and Boudart, M., *J. Catal.* **30**, 146 (1973).
14. Bird, R. B., Stewart, W. E., and Lightfoot, E. N., "Transport Phenomena." Wiley, New York, 1960.
15. Fogler, H. S., "Elements of Chemical Reaction Engineering." Prentice Hall, New York, 1992.
16. Treybal, R. E., "Mass-Transfer Operations." McGraw-Hill, New York, 1980.
17. Chou, P., and Vannice, M. A., *J. Catal.* **105**, 342 (1987).
18. Lombardo, S. J., and Bell, A. T., *Surf. Sci. Reports* **13**, 1 (1991).
19. Abderrahim, H., and Duprez, D., *Studies Surf. Sci. Catal.* **30**, 359 (1987).
20. Martin, D., and Duprez, D., *J. Phys. Chem.* **100**, 9429 (1996).